Bound states for truncated Coulomb potentials

2000 J. Phys. A: Math. Gen. 33 7013

(http://iopscience.iop.org/0305-4470/33/39/316)

J. Phys. A: Math. Gen. **33** (2000) 7013–7023. Printed in the UK PII: S0305-4470(00)14440-3

Bound states for truncated Coulomb potentials

Maen Odeh and Omar Mustafa

Department of Physics, Eastern Mediterranean University, G Magusa, North Cyprus, Mersin 10, Turkey

E-mail: maen.odeh@emu.edu.tr and omar.mustafa@emu.edu.tr

Received 28 April 2000

Abstract. The pseudoperturbative shifted-l expansion technique (PSLET) is generalized for states with an arbitrary number of nodal zeros. Bound-states energy eigenvalues for two truncated Coulombic potentials are calculated using PSLET. In contrast with the shifted large-N expansion technique, PSLET results compare excellently with those from a direct numerical integration.

(Some figures in this article are in colour only in the electronic version; see www.iop.org)

1. Introduction

Attractive truncated Coulomb potentials

$$V(r) = -\frac{1}{(r^b + \alpha^b)^{1/b}} \tag{1}$$

($b = 1, 2, 3, \ldots$ and α is a truncation parameter) are of particular physical interest. They avoid the singularity at $r = 0$ (the crux of divergence problems) and serve as models for many interesting physical phenomena [1–10]. For the case $b = 1$, equation (1) reads

$$V(r) = -\frac{1}{(r + \alpha)} \tag{2}$$

the eminent cut-off Coulomb potential. In quantum-field theory, it has been suggested that if gravitational interactions of elementary particles are taken into account, there would be a gravitational cut-off of Coulomb interactions resulting in a finite theory for the quantum field. Equation (2) therefore represents a non-relativistic version of this idea. It may, moreover, be considered as an approximation of the potential of a smeared charge rather than a point charge. When $b = 2$, equation (1) implies

$$V(r) = -\frac{1}{(r^2 + \alpha^2)^{1/2}} \tag{3}$$

often called the laser-dressed Coulomb potential. A model that has been found to be useful for the study of the spectrum of a laser-dressed hydrogen-like atoms when exposed to an intense non-resonant laser-field [5–10]. It has been shown that under Kramers–Henneberger canonical transformations the potential of such atoms can be recast as (3) with the truncation parameter α being related to the strength of the irradiating laser field [7–9]. The effective potential for scattering by a uniform spherical charge distribution is well simulated by (3). Moreover, it is

0305-4470/00/397013+11$30.00

very similar to the modified potential of the nucleus of a muonic atom due to its finite size [5, 11–15].

As the Schrödinger equation for neither of the potentials is amenable to a general analytic solution, one has to use perturbation techniques or numerical methods to analyse their bound states. Mehta and Patil [2] had investigated analytically the s-state energy for the potential (2); however, no numerical results were obtained. Intensive analyses had been carried out by De Meyer and Vanden Berghe [3] and Fernandez [4] on the bound states of (2). The shifted $1/N$ expansion technique had been employed to calculate the energy eigenvalues of potential (3) [6]. Singh *et al* [5] have employed a numerical method to calculate the energy eigenvalues for potentials (2) and (3). As such, these potentials are good candidates for analysis through an analytical (often semi-analytical) technique to resolve their underlying physical aspects.

Recently, we have introduced a pseudoperturbative shifted-l (l is the angular momentum quantum number) expansion technique (PSLET) to solve for nodeless states of the Schrödinger equation. It simply consists of using $1/\bar{l}$ as a pseudoperturbation parameter, where $\bar{l} = l - \beta$, and β is a suitable shift. The shift β is vital as it removes the poles that would emerge, at lowest orbital states with $l = 0$, in our proposed expansion below. Our new analytical, often semi-analytical, methodical proposal for PSLET has been applied successfully to a quasi-relativistic harmonic oscillator [16], spiked harmonic oscillator [17], anharmonic oscillators [18] and two-dimensional hydrogenic atom in an arbitrary magnetic field [19].

Encouraged by its satisfactory performance in handling nodeless states, we generalize the PSLET recipe (in section 2) to states with an arbitrary number of nodal zeros, $n_r \geqslant 0$. In section 3 we apply PSLET to treat potentials (2) and (3) and we compare the results obtained by PSLET with the exact ones. We conclude in section 4.

2. Method

The prescription of our technique starts with the radial part of the time-independent Schrödinger equation (in units where $\hbar = m = 1$),

$$\left[-\frac{1}{2}\frac{\mathrm{d}^2}{\mathrm{d}r^2} + \frac{l(l+1)}{2r^2} + V(r)\right]\Psi_{n_r,l}(r) = E_{n_r,l}\Psi_{n_r,l}(r) \tag{4}$$

where l is the angular momentum quantum number, $n_r = 0, 1, \ldots$ counts the nodal zeros and $V(r)$ is an arbitrary spherically symmetric potential that supports bound states.

Most textbook perturbation techniques manipulate the potential term to introduce a perturbating expansion parameter. In contrast, our method keeps the potential arbitrary with the condition of being well behaved. We use the centrifugal term to play this role. Thus, with $\bar{l} = l - \beta$ (β to be determined in the following), equation (4) reads

$$\left\{-\frac{1}{2}\frac{\mathrm{d}^2}{\mathrm{d}r^2} + \frac{\bar{l}^2 + (2\beta+1)\bar{l} + \beta(\beta+1)}{2r^2} + V(r)\right\}\Psi_{n_r,l}(r) = E_{n_r,l}\Psi_{n_r,l}(r). \tag{5}$$

Apparently, the natural limit of equation (5) is the large-l limit. In that limit the centrifugal term dominates over the kinetic energy and the potential terms. This results in a semiclassical motion of the particle in an effective potential $V_{\mathrm{eff}} = \frac{1}{2r^2} + \frac{1}{Q}V(r)$, where Q is a constant that scales the potential in the large-l limit and is set, for any specific choice of l and n_r, equal to $\bar{l}^2$ at the end of calculations [19, 20]. Hence, the motion is concentrated about the minimum of V_{eff}, say r_0. Consequently, a coordinate transformation through

$$x = \bar{l}^{1/2}(r - r_0)/r_0 \tag{6}$$

will be used. It is worth mentioning that the scaled coordinates, equation (6), have no effect on the energy eigenvalues, which are coordinate independent. They just facilitate the calculation of both the energy eigenvalues and eigenfunctions. Performing the coordinate transformation, equations (6) and (5) read

$$\left[-\frac{1}{2}\frac{\mathrm{d}^2}{\mathrm{d}x^2}+\frac{r_0^2}{\bar{l}}\tilde{V}(x(r))\right]\Psi_{n_r,l}(x)=\frac{r_0^2}{\bar{l}}E_{n_r,l}\Psi_{n_r,l}(x) \tag{7}$$

$$\tilde{V}(x(r))=\frac{\bar{l}^2+(2\beta+1)\bar{l}+\beta(\beta+1)}{2r_0^2\left(1+x/\sqrt{\bar{l}}\right)^2}+\frac{\bar{l}^2}{Q}V(x(r)). \tag{8}$$

Expansions about $x=0$, i.e. $r=r_0$, yield

$$\frac{1}{r_0^2\left(1+x/\sqrt{\bar{l}}\right)^2}=\sum_{n=0}^{\infty}(-1)^n\frac{(n+1)}{r_0^2}x^n\bar{l}^{-n/2} \tag{9}$$

$$V(x(r))=\sum_{n=0}^{\infty}\left(\frac{\mathrm{d}^nV(r_0)}{\mathrm{d}r_0^n}\right)\frac{(r_0x)^n}{n!}\bar{l}^{-n/2}. \tag{10}$$

Apparently, the expansions in (9) and (10) centre the problem at the point r_0 and the derivatives, in effect, contain information not only at r_0 but also at any point on the axis, in accordance with Taylor's theorem. It is also convenient to expand E as

$$E_{n_r,l}=\sum_{n=-2}^{\infty}E_{n_r,l}^{(n)}\bar{l}^{-n}. \tag{11}$$

Equation (7) thus becomes

$$\left[-\frac{1}{2}\frac{\mathrm{d}^2}{\mathrm{d}x^2}+\frac{r_0^2}{\bar{l}}\tilde{V}(x(r))\right]\Psi_{n_r,l}(x)=r_0^2\left(\sum_{n=-2}^{\infty}E_{n_r,l}^{(n)}\bar{l}^{-(n+1)}\right)\Psi_{n_r,l}(x) \tag{12}$$

with

$$\begin{aligned}\frac{r_0^2}{\bar{l}}\tilde{V}(x(r))=r_0^2\bar{l}&\left[\frac{1}{2r_0^2}+\frac{V(r_0)}{Q}\right]+\bar{l}^{1/2}\left[-x+\frac{V'(r_0)r_0^3x}{Q}\right]\\&+\left[\frac{3}{2}x^2+\frac{V''(r_0)r_0^4x^2}{2Q}\right]+(2\beta+1)\sum_{n=1}^{\infty}(-1)^n\frac{(n+1)}{2}x^n\bar{l}^{-n/2}\\&+r_0^2\sum_{n=3}^{\infty}\left[(-1)^n\frac{(n+1)}{2r_0^2}x^n+\left(\frac{\mathrm{d}^nV(r_0)}{\mathrm{d}r_0^n}\right)\frac{(r_0x)^n}{n!Q}\right]\bar{l}^{-(n-2)/2}\\&+\beta(\beta+1)\sum_{n=0}^{\infty}(-1)^n\frac{(n+1)}{2}x^n\bar{l}^{-(n+2)/2}+\frac{(2\beta+1)}{2}\end{aligned} \tag{13}$$

where the prime of $V(r_0)$ denotes a derivative with respect to r_0. Equation (12) is exactly of the type of Schrödinger equation for one-dimensional anharmonic oscillator

$$\left[-\frac{1}{2}\frac{\mathrm{d}^2}{\mathrm{d}x^2}+\frac{1}{2}\Omega^2x^2+\xi_0+P(x)\right]X_{n_r}(x)=\lambda_{n_r}X_{n_r}(x) \tag{14}$$

where $P(x)$ is a perturbation-like term and ξ_0 is a constant. A simple comparison between equations (12)–(14) implies

$$\xi_0 = \bar{l}\left[\frac{1}{2} + \frac{r_0^2 V(r_0)}{Q}\right] + \frac{2\beta+1}{2} + \frac{\beta(\beta+1)}{2\bar{l}} \tag{15}$$

$$\lambda_{n_r} = \bar{l}\left[\frac{1}{2} + \frac{r_0^2 V(r_0)}{Q}\right] + \left[\frac{2\beta+1}{2} + \left(n_r + \frac{1}{2}\right)\Omega\right] + \frac{1}{\bar{l}}\left[\frac{\beta(\beta+1)}{2} + \lambda_{n_r}^{(0)}\right] + \sum_{n=2}^{\infty} \lambda_{n_r}^{(n-1)} \bar{l}^{-n} \tag{16}$$

and

$$\lambda_{n_r} = r_0^2 \sum_{n=-2}^{\infty} E_{n_r,l}^{(n)} \bar{l}^{-(n+1)}. \tag{17}$$

Equations (15) and (16) yield

$$E_{n_r,l}^{(-2)} = \frac{1}{2r_0^2} + \frac{V(r_0)}{Q} \tag{18}$$

$$E_{n_r,l}^{(-1)} = \frac{1}{r_0^2}\left[\frac{2\beta+1}{2} + (n_r + \frac{1}{2})\Omega\right] \tag{19}$$

$$E_{n_r,l}^{(0)} = \frac{1}{r_0^2}\left[\frac{\beta(\beta+1)}{2} + \lambda_{n_r}^{(0)}\right] \tag{20}$$

$$E_{n_r,l}^{(n)} = \lambda_{n_r}^{(n)}/r_0^2 \qquad n \geqslant 1. \tag{21}$$

Here r_0 is chosen to minimize $E_{n_r,l}^{(-2)}$, i.e.

$$\frac{\mathrm{d}E_{n_r,l}^{(-2)}}{\mathrm{d}r_0} = 0 \qquad \text{and} \qquad \frac{\mathrm{d}^2 E_{n_r,l}^{(-2)}}{\mathrm{d}r_0^2} > 0 \tag{22}$$

which in turn gives, with $\bar{l} = \sqrt{Q}$,

$$l - \beta = \sqrt{r_0^3 V'(r_0)}. \tag{23}$$

Consequently, the second term in equation (13) vanishes and the first term adds a constant to the energy eigenvalues. It should be noted that energy term $\bar{l}^2 E_{n_r,l}^{(-2)}$ is the energy of a particle moving under the effect of V_{eff}. Hence, it is roughly the energy of a classical particle with angular momentum $L_z = \bar{l}$ executing circular motion of radius r_0 in the potential $V(r_0)$. This term thus identifies the leading-order approximation, to all eigenvalues, as a classical approximation and the higher-order corrections as quantum fluctuations around the minimum r_0, organized in inverse powers of $\bar{l}$.

The next leading correction to the energy series, $\bar{l} E_{n_r,l}^{(-1)}$, consists of a constant term and the exact eigenvalues of the unperturbed harmonic oscillator potential $\Omega^2 x^2/2$. The shifting parameter β is determined by choosing $\bar{l} E_{n_r,l}^{(-1)} = 0$. This choice is physically motivated. It requires not only agreement between PSLET eigenvalues and the exact known ones for the harmonic oscillator and Coulomb potentials but also between the eigenfunctions as well. Hence

$$\beta = -\left[\frac{1}{2} + \left(n_r + \frac{1}{2}\right)\Omega\right] \tag{24}$$

where

$$\Omega = \sqrt{3 + \frac{q_0 V''(r_0)}{V'(r_0)}}. \tag{25}$$

Equation (13) thus becomes

$$\frac{r_0^2}{\bar{l}} \tilde{V}(x(r)) = r_0^2 \bar{l} \left[\frac{1}{2r_0^2} + \frac{V(r_0)}{Q} \right] + \sum_{n=0}^{\infty} v^{(n)}(x) \bar{l}^{-n/2} \tag{26}$$

where

$$v^{(0)}(x) = \frac{1}{2}\Omega^2 x^2 + \frac{2\beta + 1}{2} \tag{27}$$

$$v^{(1)}(x) = -(2\beta + 1)x - 2x^3 + \frac{r_0^5 V'''(r_0)}{6Q} x^3 \tag{28}$$

and for $n \geqslant 2$

$$v^{(n)}(x) = (-1)^n (2\beta + 1) \frac{(n+1)}{2} x^n + (-1)^n \frac{\beta(\beta+1)}{2} (n-1) x^{(n-2)} + B_n x^{n+2} \tag{29}$$

$$B_n = (-1)^n \frac{(n+3)}{2} + \frac{r_0^{(n+4)}}{Q(n+2)!} \frac{\mathrm{d}^{n+2} V(r_0)}{\mathrm{d} r_0^{n+2}}. \tag{30}$$

Equation (12) thus becomes

$$\left[-\frac{1}{2} \frac{\mathrm{d}^2}{\mathrm{d}x^2} + \sum_{n=0}^{\infty} v^{(n)} \bar{l}^{-n/2} \right] \Psi_{n_r,l}(x) = r_0^2 \left[\sum_{n=1}^{\infty} E_{n_r,l}^{(n-1)} \bar{l}^{-n} \right] \Psi_{n_r,l}(x). \tag{31}$$

Up to this point, one would conclude that the above procedure is nothing but an animation of the eminent shifted large-N expansion (SLNT) [20, 21]. However, because of the limited capabilities of SLNT in handling large-order corrections via the standard Rayleigh–Schrödinger perturbation theory, only low-order corrections have been reported, sacrificing in effect its preciseness. Therefore, one should seek an alternative and proceed by setting the wavefunctions with any number of nodes as

$$\Psi_{n_r,l}(x) = F_{n_r,l}(x) \exp(U_{n_r,l}(x)). \tag{32}$$

Equation (31) is readily transformed into the following Riccati-type equation:

$$-\frac{1}{2} \left[F''_{n_r,l}(x) + 2F'_{n_r,l}(x) U'_{n_r,l}(x) \right] + F_{n_r,l}(x) \left\{ -\frac{1}{2} \left[U''_{n_r,l}(x) + (U'_{n_r,l}(x))^2 \right] \right.$$
$$\left. + \frac{1}{2}(2\beta + 1) + \frac{1}{2}\Omega^2 x^2 + \sum_{n=1}^{\infty} v^{(n)}(x) \bar{l}^{-n/2} \right\} = r_0^2 F_{n_r,l}(x) \sum_{n=1}^{\infty} E_{n_r,l}^{(n-1)} \bar{l}^{-n} \tag{33}$$

where primes denotes derivatives with respect to x. It is evident that (33) admits solutions of the form

$$F_{n_r,l}(x) = x^{n_r} + \sum_{n=0}^{\infty} \sum_{p=0}^{n_r - 1} a_{p,n_r}^{(n)} x^p \bar{l}^{-n/2} \tag{34}$$

$$U'_{n_r,l}(x) = \sum_{n=0}^{\infty} U_{n_r}^{(n)}(x) \bar{l}^{-n/2} + \sum_{n=0}^{\infty} G_{n_r}^{(n)}(x) \bar{l}^{-(n+1)/2} \tag{35}$$

where

$$U_{n_r}^{(n)}(x) = \sum_{m=0}^{n+1} D_{m,n,n_r} x^{2m-1} \qquad D_{0,n,n_r} = 0 \tag{36}$$

$$G_{n_r}^{(n)}(x) = \sum_{m=0}^{n+1} C_{m,n,n_r} x^{2m}. \tag{37}$$

Clearly, the nodal zeros of the wavefunctions are taken care of by $F_{n_r,l}(x)$. For nodeless states,

$$F_{0,l}(x) = 1 \tag{38}$$

which reduces (33) to the problem described in our previous work for nodeless states [16–19]. To illustrate how our method works for nodal states, we will treat the one-node state. Upon substituting equations (34)–(37) with $n_r = 1$ into (33), it reads

$$\begin{aligned} F_{1,l}(x)\Bigg[& -\frac{1}{2}\sum_{n=0}^{\infty}\left(U_1^{(n)'}(x)\bar{l}^{-n/2} + G_1^{(n)'}(x)\bar{l}^{-(n+1)/2}\right) \\ & -\frac{1}{2}\sum_{n=0}^{\infty}\sum_{m=0}^{n}\Bigg(U_1^{(m)}(x)U_1^{(n-m)}(x)\bar{l}^{-n/2} + G_1^{(m)}(x)G_1^{(n-m)}(x)\bar{l}^{-(n+2)/2} \\ & +2U_1^{(m)}(x)G_1^{(n-m)}(x)\bar{l}^{-(n+1)/2}\Bigg) + \sum_{n=0}^{\infty} v^{(n)}(x)\bar{l}^{-n/2} - r_0^2\sum_{n=1}^{\infty} E_{n_r,l}^{(n-1)}\bar{l}^{-n}\Bigg] \\ & -F'_{1,l}(x)\left(\sum_{n=0}^{\infty} U_{n_r}^{(n)}(x)\bar{l}^{-n/2} + \sum_{n=0}^{\infty} G_{n_r}^{(n)}(x)\bar{l}^{-(n+1)/2}\right) - \frac{1}{2}F''_{1,l}(x) = 0. \end{aligned} \tag{39}$$

The solution of (39) then follows from the uniqueness of the power-series representation. Therefore, equating the coefficients of the same powers of $\bar{l}$ and x, respectively (of course, the other way around works equally well), one obtains

$$D_{1,0,1} = -\omega \qquad a_{0,1}^{(0)} = 0 \qquad U_1^{(0)}(x) = -\omega x \tag{40}$$

$$C_{1,0,1} = -\frac{B_1}{\omega} \qquad a_{0,1}^{(1)} = -\frac{C_{1,0,1}}{\omega} \tag{41}$$

$$C_{0,0,1} = \frac{1}{\omega}(2C_{1,0,1} + 2\beta + 1) \tag{42}$$

$$D_{2,2,1} = \frac{1}{\omega}\left(\frac{C_{0,0,1}^2}{\omega} - B_2\right) \tag{43}$$

$$D_{1,2,1} = \frac{1}{\omega}\left(\frac{5}{2}D_{2,2,1} + C_{0,0,1}C_{1,0,1} - \frac{3}{2}(2\beta+1),\right) \tag{44}$$

$$E_{1,l}^{(0)} = \frac{1}{r_0^2}\left(\beta(\beta+1) + a_{0,1}^{(1)}C_{1,0,1} - \frac{3D_{1,2,1}}{2} - \frac{C_{0,0,1}^2}{2}\right) \tag{45}$$

and so on. Obviously, one can calculate the energy eigenvalue and eigenfunctions from the knowledge of C_{m,n,n_r}, D_{m,n,n_r} and $a_{p,n_r}^{(n)}$ in a hierarchical manner. Nevertheless, the procedure just described is suitable for a software package such as MAPLE to determine the energy eigenvalue and eigenfunction up to any order of the pseudoperturbation series.

Although the energy series equation (11), could appear divergent, or at best, asymptotic for small $\bar{l}$, one can still calculate the eigenseries to a very good accuracy by performing the sophisticated $[N, M]$ Padé approximation [22],

$$P_N^M(1/\bar{l}) = \frac{\left(P_0 + P_1/\bar{l} + \cdots + P_M/\bar{l}^N\right)}{\left(1 + q_1/\bar{l} + \cdots + q_N/\bar{l}^M\right)} \tag{46}$$

to the energy series, equation (11). The energy series, equation (11), is calculated up to $E^{(8)}_{n_r,l}/\bar{l}^8$ by

$$E_{n_r,l} = \bar{l}^2 E^{(-2)}_{n_r,l} + E^{(0)}_{n_r,l} + \cdots + E^{(8)}_{n_r,l}/\bar{l}^8 + \mathrm{O}(1/\bar{l}^9) \tag{47}$$

and with the $P_4^4(1/\bar{l})$ Padé approximant it becomes

$$E_{n_r,l}[4,4] = \bar{l}^2 E^{(-2)}_{n_r,l} + P_4^4(1/\bar{l}). \tag{48}$$

Our technique is therefore well prescribed.

3. Truncated Coulomb potentials

In this section we consider the truncated Coulomb potentials, equations (2) and (3).

Substituting equation (2) into equation (25), one obtains

$$\Omega = \sqrt{\frac{r_0 + 3\alpha}{r_0 + \alpha}}. \tag{49}$$

Equation (23) together with equation (24) then give

$$l + \frac{1}{2}\left[1 + (2n_r + 1)\sqrt{\frac{r_0 + 3\alpha}{r_0 + \alpha}}\right] = \frac{r_0^{3/2}}{(r_0 + \alpha)}. \tag{50}$$

On substituting equation (3) into equation (25), one obtains

$$\Omega = \sqrt{\frac{r_0^2 + 4\alpha^2}{r_0^2 + \alpha^2}}. \tag{51}$$

Equation (23) in turn gives

$$l + \frac{1}{2}\left[1 + (2n_r + 1)\sqrt{\frac{r_0^2 + 4\alpha^2}{r_0^2 + \alpha^2}}\right] = \frac{r_0^2}{(r_0 + \alpha)^{3/4}}. \tag{52}$$

Equations (50) and (52) are explicit equations in r_0. Clearly, closed-form solutions of equations (49)–(51) for r_0 are hard to find (which is often the case). Thus, we use numerical methods to resolve the issue (hence the notion that PSLET is often semianalytical). Once r_0 is determined the coefficients C_{m,n,n_r}, D_{m,n,n_r}, $a^{(n)}_{p,n_r}$ are determined in a sequential manner. Hence the eigenvalues, equation (47), and eigenfunctions equations (34)–(37), are calculated in the same batch for each value of l, n_r and α.

Tables 1 and 2 show PSLET results, equation (47), E_{PSLET}, for 1s, 2s, 2p, 3p, 3d, 4d and 4f eigenstates of equation (1), covering weak, intermediate and strong ranges of the truncation parameter α. In addition, we display the Padé approximants, equation (48), $E[4, 4]$, and the exact results, E_{exact}, obtained by direct numerical integration [5]. Comparing E_{PSLET} with E_{exact}, one notes the underlying relation between the accuracy of the PSLET results and l, n_r

Table 1. Bound-state energies (in units where $\hbar = m = 1$) of the potential $V(r) = -\frac{1}{(r+\alpha)}$ for the 1s, 2s, 2p and 3p states. E_{PSLET} represents PSLET results, equation (47), E_{44} is the [4, 4] Padé approximant, equation (48) and E_{exact} from direct numerical integration [5].

	α	1s	2s	2p	3p
$-E_{\mathrm{PSLET}}$		0.387 357 746	0.109 481 497	0.117 535 370	0.053 309 085
$-E_{44}$	0.1	0.387 922 157	0.109 145 059	0.117 535 388	0.053 309 210
$-E_{\mathrm{exact}}$		0.387 543 65	0.109 508 05	0.117 535 35	0.053 309 30
		0.180 406 651	0.069 577 091	0.082 862 488	0.041 787 781
	1.0	0.180 368 972	0.069 581 801	0.082 862 452	0.041 787 655
		0.180 367 05	0.069 580 66	0.082 862 42	0.041 787 66
		0.043 439 053	0.024 810 349	0.029 446 519	0.018 748 152
	10	0.043 438 645	0.024 810 342	0.029 446 516	0.018 748 153
		0.043 438 72	0.024 810 36	0.029 446 52	0.018 798 15
		0.012 194 732	0.008 579 236	0.009 717 589	0.007 237 436
	50	0.012 194 683	0.008 579 235	0.009 717 588	0.007 237 436
		0.012 194 69	0.008 579 24	0.009 717 59	0.007 237 44
		0.003 653 176	0.002 907 080	0.003 169 533	0.002 608 781
	200	0.003 653 168	0.002 907 080	0.003 169 533	0.002 608 781
		0.003 653 17	0.002 907 08	0.003 169 53	0.002 608 78

Table 2. Bound-state energies (in units where $\hbar = m = 1$) of the potential $V(r) = -\frac{1}{(r+\alpha)}$ for the 3d, 4d and 4f states. E_{PSLET} represents PSLET results, equation (47), E_{44} is the [4, 4] Padé approximant, equation (48) and E_{exact} from direct numerical integration [5].

	α	3d	4d	4f
$-E_{\mathrm{PSLET}}$		0.054 136 568	0.030 648 450	0.030 813 599
$-E_{44}$	0.1	0.054 136 568	0.030 648 449	0.030 813 599
$-E_{\mathrm{exact}}$		0.054 136 57	0.030 648 45	0.030 813 60
		0.045 010 006	0.026 625 065	0.027 588 160
	1.0	0.045 010 007	0.026 625 059	0.027 588 160
		0.045 010 01	0.026 625 06	0.027 588 16
		0.021 024 302	0.014 373 461	0.015 576 600
	10	0.021 024 302	0.014 373 461	0.015 576 600
		0.021 024 30	0.014 373 46	0.015 576 60
		0.007 962 796	0.006 153 630	0.006 643 882
	50	0.007 962 796	0.006 153 630	0.006 643 882
		0.007 962 80	0.006 153 63	0.006 643 88
		0.002 798 562	0.002 353 647	0.002 498 272
	200	0.002 798 562	0.002 353 647	0.002 498 272
		0.002 798 56	0.002 353 65	0.002 498 27

and the truncation parameter, α. The accuracy of the PSLET results increases with increasing l and/or n_r (see figure 2). This is in accordance with our choice for the expansion parameter in equation (47), as $1/\bar{l}$ becomes smaller as l and/or n_r increases. The PSLET results show a good converging trend to the exact values as the truncation parameter becomes larger (see figure 1). In the strong range of α, the PSLET results are almost exact. To resum the eigenenergy series, equation (47), the Padé approximant is calculated. Moreover, the stability noted in different

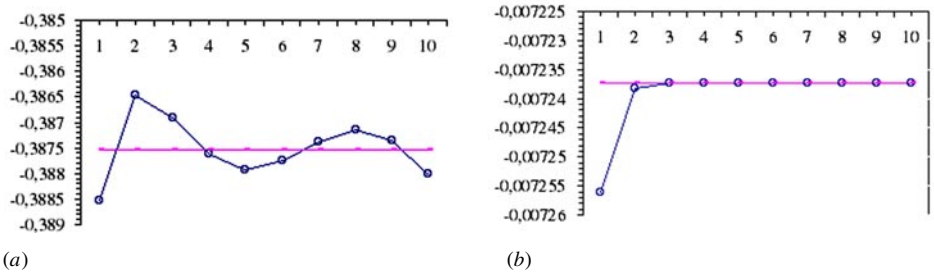

(*a*) (*b*)

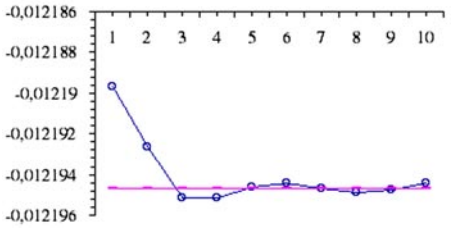

(*c*)

Figure 1. The effect of the truncation parameter on the trend of convergence of equation (47) for 1s-state of equation (2): (*a*) $\alpha = 0.1$, (*b*) $\alpha = 50$, (*c*) $\alpha = 200$. Where the numbers on the horizontal axis represent the number of corrections added to the leading energy term of PSLET, equation (47), the vertical axis represents the energies ($\hbar = m = 1$) and the horizontal curve denotes the exact numerical results from [5].

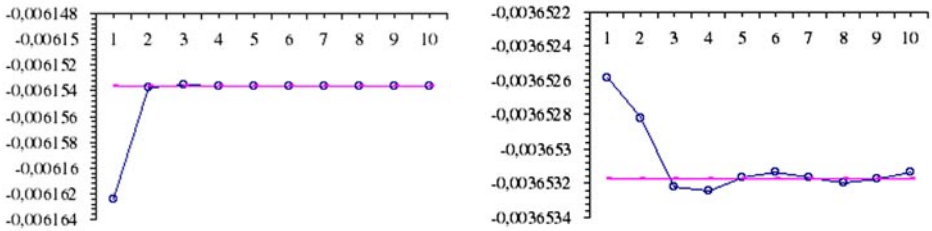

(*a*) (*b*)

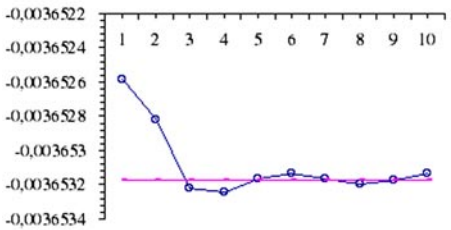

(*c*)

Figure 2. The effect of the angular momentum quantum number, l, and the radial quantum number, n_r, on the convergence trend of equation (47) for (2) with $\alpha = 50$: (*a*) 1s-state, (*b*) 3p-state, (*c*) 4d-state. Symbols as in figure 1.

order Padé approximants shows that the results are accurate up to ten digits in the strong range of α, in contrast to the results obtained in [5] where the accuracy is recorded up to eight digits over the same range.

Table 3 displays the PSLET results, E_{PSLET}, for some excited states of equation (3) along with the Padé approximants, $E[4, 4]$, of E_{PSLET}, the results obtained by SLNT [6], E_{SLNT} and the exact results, E_{exact}, obtained by direct numerical integration [5]. Apparently, the accuracy of our results for this potential has similar behaviour to the previous case. When compared with the results obtained by SLNT, our results show better agreement with the exact ones. The difficulty in calculating high-order corrections in SLNT through Rayleigh–Schrödinger perturbation theory results in a loss in accuracy. PSLET makes it possible to calculate high-order corrections which improves the accuracy.

Table 3. Bound-state energies (in units where $\hbar = m = 1$) of the potential $V(r) = -\frac{1}{(r^2+\alpha^2)^{1/2}}$ for the 3d, 4d and 4f states. E_{PSLET} represents PSLET results, equation (47), E_{44} is the [4, 4] Padé approximant, equation (48) E_{SLNT} is from SLNT [6] and E_{exact} from direct numerical integration [5].

	α	2s	3p	4d
$-E_{\mathrm{PSLET}}$		0.121 234 415	0.055 496 250	0.031 244 807
$-E_{44}$	0.1	0.126 937 229	0.055 498 046	0.031 244 799
$-E_{\mathrm{SLNT}}$	—	—	—	—
$-E_{\mathrm{exact}}$		0.121 820 90	0.055 495 23	0.031 244 80
		0.089 679 150	0.052 114 869	0.030 781 155
	1.0	0.095 048 845	0.052 110 018	0.030 781 125
		0.089 903	0.052 509	0.030 838
		0.092 679 33	0.052 060 38	0.030 781 50
		0.037 161 915	0.028 313 951	0.021 412 017
	10	0.037 154 303	0.028 313 599	0.021 412 537
		0.037 111	0.028 225	0.021 353
		0.037 154 40	0.028 313 69	0.021 412 57
		0.012 450 958	0.010 878 999	0.009 476 019
	50	0.012 450 960	0.010 879 000	0.009 476 018
		0.016 263	0.010 882	0.009 477
		0.012 450 96	0.010 879 00	0.009 476 02
		0.003 923 030	0.003 659 489	0.003 410 238
	200	0.003 923 030	0.003 659 489	0.003 410 238
		0.004 503	0.003 660	0.003 411
		0.003 923 03	0.003 659 49	0.003 410 24

Moreover, one notes that the results of PSLET are more accurate in the case of the truncated Coulomb potential than that of the laser-dressed one. The reason behind this is that the truncated potential is more Coulombic in nature which makes PSLET nearer to the exact results.

4. Concluding remarks

We have presented a generalization of our pseudoperturbative shifted-l expansion technique PSLET [16–19] to treat states with an arbitrary number of nodal zeros, $n_r \geqslant 0$. Two truncated Coulombic potentials have been treated via PSLET and very accurate energy eigenvalues have been obtained.

The outstanding features of the attendant PSLET are that it avoids troublesome questions such as those pertaining to the nature of small-parameter expansions, the trend of convergence to the exact numerical values (noted in tables 1–3), the utility in calculating the eigenvalues and eigenfunctions in one batch to sufficiently higher orders and applicability to a wide range of potentials. Moreover, beyond its promise of being quite handy, on computational and practical methodical sides, it offers a useful perturbation prescription where the zeroth-order approximation inherits a substantial amount of the total energy.

Finally, the scope of PSLET applicability extends beyond the present truncated Coulombic potentials. It could be applied to angular momentum states of multi-electron atoms [23–25], relativistic and non-relativistic quark–antiquark models [26], etc. We believe that the feature of our method in determining expressions for the bound-state wavefunctions makes it possible

to describe electron transitions and multiphoton emission occurring in atomic systems in the presence of an intense laser field. It is therefore reasonable to re-examine such phenomena within the framework of PSLET.

References

[1] Patil H 1981 *Phys. Rev.* A **24** 2913
[2] Mehta H and Patil H 1978 *Phys. Rev.* A **17** 43
[3] De Meyer H and Berghe G V 1990 *J. Phys. A: Math. Gen.* **23** 1323
[4] Fernandez F M 1991 *J. Phys. A: Math. Gen.* **24** 1351
[5] Singh D, VarshniY P and Dutt R 1985 *Phys. Rev.* A **32** 619
[6] Dutt R, Mukherji U and Varshni Y P 1985 *J. Phys. B: At. Mol. Phys.* **18** 3311 and references therein
[7] Miranda L C 1981 *Phys. Lett.* A **86** 363
[8] Lima C A and Miranda L C 1981 *Phys. Lett.* A **86** 367
[9] Lima C A and Miranda L C 1981 *Phys. Rev.* A **23** 3335
[10] Landgraf T C *et al* 1982 *Phys. Lett.* A **92** 131
[11] Landau L 1956 *Niels Bohr and the Development of Physics* (London: Pergamon)
Klein O 1956 *Niels Bohr and the Development of Physics* (London: Pergamon)
[12] Pauli W 1956 *Helv. Phys. Acta. Suppl.* **4** 69
[13] Deser S 1957 *Rev. Mod. Phys.* **29** 417
[14] Isham C J, Salam A and Strathdee J 1971 *Phys. Rev.* D **3** 1805
Isham C J, Salam A and Strathdee J 1972 **5** 2548
[15] Marshak R E 1952 *Meson Physics* (New York: Dover)
[16] Mustafa O and Odeh M 1999 *J. Phys. A: Math. Gen.* **32** 6653
[17] Mustafa O and Odeh M 1999 *J. Phys. B: At. Mol. Opt. Phys.* **32** 3055
[18] Mustafa O and Odeh M 2000 *Eur. Phys. J.* B at press
[19] Mustafa O and Odeh M 2000 *Commun. Theor. Phys.* **33** 469
[20] Imbo T, Pagnamenta A and Sukhmate U 1984 *Phys. Rev.* D **29** 1669
[21] Maluendes S A, Fernandez F M and Castro E A 1989 *Phys. Lett.* A **39** 1605
[22] Bender C M and Orszag S A 1978 *Advanced Mathematical Methods for Scientists and Engineers* (New York: McGraw-Hill)
[23] Dunn M and Watson D 1996 *Few-Body Syst.* **21** 187
[24] Dunn M and Watson D 1996 *Ann. Phys.* **251** 266
[25] Dunn M and Watson D 1999 *Phys. Rev.* A **59** 1109
[26] Lichtenberg D *et al* 1990 *Z. Phys.* C **46** 75